Quantum Monte Carlo calculations in the nuclear shell model by the complex Langevin method

Yuhma Asano[a,b,1], Yuta Ito[c,2], Jun Nishimura[d,e,3], and Noritaka Shimizu[f,4]

[a]*Institute of Pure and Applied Sciences, University of Tsukuba,*
1-1-1 Tennodai, Tsukuba, Ibaraki 305-8571, Japan
[b]*Tomonaga Center for the History of the Universe, University of Tsukuba,*
1-1-1 Tennodai, Tsukuba, Ibaraki 305-8571, Japan
[c]*National Institute of Technology, Tokuyama College,*
Gakuendai, Shunan, Yamaguchi 745-8585, Japan
[d]*KEK Theory Center, High Energy Accelerator Research Organization,*
1-1 Oho, Tsukuba, Ibaraki 305-0801, Japan
[e]*Graduate Institute for Advanced Studies, SOKENDAI,*
1-1 Oho, Tsukuba, Ibaraki 305-0801, Japan
[f]*Center for Computational Sciences, University of Tsukuba,*
1-1-1 Tennodai, Tsukuba, Ibaraki 305-8571, Japan

Abstract

The nuclear shell model is known to describe the properties of various nuclei extremely well. However, the auxiliary-field quantum Monte Carlo calculations cannot be applied to it with general interactions due to the sign problem. The model has therefore been investigated primarily by variational methods, where the accuracy of the results depends crucially on the ansatz for the wave function. Here we perform the auxiliary-field quantum Monte Carlo calculations in the case of small systems at finite temperature using the complex Langevin method (CLM), which has been successfully applied to various interesting systems with the sign problem over the decade. In particular, we show the existence of a parameter region in which the validity criterion for the CLM is satisfied and the expectation value of the energy obtained by exact diagonalization is correctly reproduced. Thus the CLM can be a complementary approach to the variational method for large systems.

[1]asano@het.ph.tsukuba.ac.jp

[2]y-itou@tokuyama.ac.jp

[3]jnishi@post.kek.jp

[4]shimizu@nucl.ph.tsukuba.ac.jp

arXiv:2508.15116v1 [nucl-th] 20 Aug 2025

Contents

1 Introduction

The nuclear shell model is one of the most powerful theoretical models that describe not only low-lying energy spectra of nuclei including those near the neutron drip line [1–3] but also thermal nuclear properties [4]. In this model, a frozen inert core is assumed and active particles in the valence orbits are treated by the so-called model space. The quantum many-body problem of the active particles is then solved by diagonalizing the Hamiltonian matrix in the subspace spanned by a huge number of Slater determinants, each of which represents how the active particles occupy the single-particle states. However, the dimension of the Hamiltonian matrix increases combinatorially as the active particles and the single-particle states increase in number. While the conventional Lanczos diagonalization method can handle the system with the so-called M-scheme for dimension up to $O(10^{11})$ [5], the explosive growth of the dimension hampers the shell-model calculations, in particular, in the heavy-mass region.

  In order to circumvent the problem of the explosive growth of the dimension, various efforts have been made. (See, for instance, Refs. [6, 7].) In 1990s, the auxiliary-field Monte Carlo (AFMC) method was introduced in the shell-model calculations. Based on this approach, which was named the shell model Monte Carlo (SMMC) method, pf-shell nuclei were studied successfully [8]. However, practical applications of the method turn out to be severely restricted by the notorious sign problem. In particular, a realistic effective interaction in the shell model, which is given, for instance, by the G-matrix theory or by the valence-space in-medium similarity renormalization group (VS-IMSRG) method

[9], cannot be used directly because of the sign problem. In order to circumvent this problem, one can prepare some artificial interaction without the sign problem and make an extrapolation [10], but such an extrapolation procedure often causes large uncertainties. This led to the common use of a schematic interaction without the sign problem instead [11, 12]. As another attempt, the constrained-path approximation was tested in sd- and pf-shell nuclei [13].

On the other hand, various attempts have been made to obtain approximate wave functions using variational approaches such as conventional particle-hole truncations, the VAMPIR method [14] and the Monte Carlo shell model [15]. While these methods are indeed useful in practical applications, they only provide us with the upper bound or the extrapolated value within the variational ansatz, and furthermore, they cannot be used for finite-temperature physics. Thus, it is still desirable to develop quantum Monte Carlo techniques, which do not have these problems of the variational approaches.

In this paper, we attempt to solve the sign problem in the shell-model calculations with realistic interactions by the complex Langevin method (CLM) [16, 17]. (See Ref. [18] for an earlier attempt using the Lipkin model.) While the method is known to have the wrong convergence problem, the conditions for the correct convergence have recently been clarified [19–28] and various new techniques to satisfy these conditions have been proposed. Based on these new developments, the CLM has been applied successfully to lattice QCD at finite density [29–38]. (See Refs. [39–41] for recent reviews.) See also Ref. [42] for an application to the Hubbard model.

We discuss two formalisms, which differ in how we treat the projection onto a fixed number of active particles. Our results for finite temperature show that the correct expectation value of energy is obtained only for sufficiently high temperature, which can be understood by the validity criterion of the CLM. In order to obtain results at lower temperature, we propose to introduce a tunable parameter in the interaction terms and to make an extrapolation using the data obtained in the parameter region in which the validity criterion of the CLM is satisfied. Thus we conclude that the CLM can be a useful approach to larger nuclei, which is complementary to the variational method. We hope that this approach is useful also in *ab initio* nuclear structure theories based on the configuration interaction method, such as the no-core shell-model method [43] and the VS-IMSRG method [9].

This paper is organized as follows. In section 2, we briefly review how the CLM works and discuss the validity criterion of the method. In section 3, we discuss how we apply the CLM to the nuclear shell model, and present our results in section 4. Section 5 is devoted to a summary and discussions. In Appendix A, we discuss how to implement the

projection onto a fixed number of active particles in one of the formalisms discussed in this paper.

2 Brief review of the complex Langevin method

In this section, we briefly review how the complex Langevin method works. For that, let us consider the integral

$$\langle \mathcal{O}(X) \rangle = \frac{1}{Z} \int dX \, \mathcal{O}(X) e^{-S(X)} \ , \qquad Z = \int dX \, e^{-S(X)} \ , \tag{2.1}$$

where X represents a set of dynamical variables and $S(X)$ represents its function. If $S(X)$ is a real function, $e^{-S(X)}/Z$ can be interpreted as a probabilistic weight so that one can numerically evaluate the integral by stochastic methods.

One of such stochastic methods is the so-called (real) Langevin method, which is based on the equivalence between the Fokker-Planck equation and the Langevin equation. Let us consider the following Fokker-Planck equation

$$\frac{\partial}{\partial t} P(X;t) = \frac{\partial}{\partial X} \left(\frac{\partial}{\partial X} - v(X) \right) P(X;t) \ , \tag{2.2}$$

where $P(X;t)$ is the probability distribution for X at time t and $v(X)$ is the drift term defined by $v(X) = -\frac{\partial S}{\partial X}$. If S is real and non-singular, the solution to the Fokker-Planck equation uniquely asymptotes to $e^{-S(X)}/Z$ in the large t limit. It is well known that this Fokker-Planck equation is equivalent to the Langevin equation

$$\frac{dx(t)}{dt} = v(x(t)) + \eta(t) \ , \tag{2.3}$$

where $\eta(t)$ is the white noise that satisfies

$$\langle \eta(t) \rangle_\eta = 0 \ , \qquad \langle \eta(t)\eta(t') \rangle_\eta = 2\delta(t - t') \ , \tag{2.4}$$

with $\langle \cdots \rangle_\eta$ being an average with respect to the white noise, which can be generated by the Gaussian distribution $\propto \exp[-\frac{1}{4}\int dt \, \eta(t)^2]$. The solution $x(t)$ to the Langevin equation then corresponds to the solution $P(X;t)$ to the Fokker-Planck equation through $P(X;t) = \langle \delta(X - x(t)) \rangle_\eta$. Thus one just needs to solve the Langevin equation for a long enough t to realize the desired probability distribution $e^{-S(X)}/Z$.

The complex Langevin method is an extension of the real Langevin method to a system with a complex-valued $S(x)$. In that case, it is natural to consider a complex version of the Langevin equation

$$\frac{dz(t)}{dt} = v(z(t)) + \eta(t) \ , \tag{2.5}$$

3

where $z(t)$ represents a set of complexified dynamical variables, $v(z) = -\frac{\partial S}{\partial z}$ represents the drift term, and $\eta(t)$ represents the real-valued white noise that satisfies (2.4). The equivalent Fokker-Planck equation can be obtained as

$$\frac{\partial}{\partial t}\mathcal{P}(Z, \bar{Z}; t) = \left\{ \frac{\partial}{\partial Z}\left(\frac{\partial}{\partial Z} - v(Z)\right) + \frac{\partial}{\partial \bar{Z}}\left(\frac{\partial}{\partial \bar{Z}} - \overline{v(Z)}\right) + 2\frac{\partial^2}{\partial Z \partial \bar{Z}} \right\} \mathcal{P}(Z, \bar{Z}; t)$$

$$= \left(\frac{\partial^2}{\partial X^2} - \frac{\partial}{\partial X}\operatorname{Re}\left[v(Z)\right] - \frac{\partial}{\partial Y}\operatorname{Im}\left[v(Z)\right] \right) \mathcal{P}(Z, \bar{Z}; t) , \tag{2.6}$$

where X and Y are the real and imaginary parts of Z, respectively, and $\mathcal{P}(Z, \bar{Z}; t)$ is the probability distribution for Z and $\bar{Z}$ at time t. If the following equation holds

$$\int dX\, P(X; t)\mathcal{O}(X) = \int dZ\, d\bar{Z}\, \mathcal{P}(Z, \bar{Z}; t)\mathcal{O}(Z) , \tag{2.7}$$

where $P(X; t)$ is a complex-valued function that satisfies (2.2) with the complex-valued $S(X)$, a solution to the complex Langevin equation (2.5) gives the expectation value of observables with the complex weight $P(X; t)$.

Let us note first that, unlike the real Langevin case, $P(X; t)$ does not necessarily converge to e^{-S}/Z. This is not a problem, however, as far as $\mathcal{P}(Z, \bar{Z}; t)$ that satisfies (2.7) converges uniquely to some finite function in the $t \to \infty$ limit since in that case, one can prove that the $t \to \infty$ limit of $P(X; t)$ should be e^{-S}/Z [23].

Thus the question boils down to whether (2.7) holds, and if so, under which condition. By formal integration of the Fokker-Planck equation (2.6), the right-hand side of (2.7) can be rewritten as [20, 21]

$$\int dZ\, d\bar{Z}\, \mathcal{P}(Z, \bar{Z}; t)\mathcal{O}(Z) = \int dZ\, d\bar{Z}\, \{e^{tL^T}\mathcal{P}(Z, \bar{Z}; 0)\}\mathcal{O}(Z) , \tag{2.8}$$

where L is the Langevin operator for (2.5) given by

$$L = \frac{\partial^2}{\partial X^2} + \operatorname{Re}\left[v(Z)\right]\frac{\partial}{\partial X} + \operatorname{Im}\left[v(Z)\right]\frac{\partial}{\partial Y} , \tag{2.9}$$

and its transpose L^T reads

$$L^T = \frac{\partial^2}{\partial X^2} - \frac{\partial}{\partial X}\operatorname{Re}\left[v(Z)\right] - \frac{\partial}{\partial Y}\operatorname{Im}\left[v(Z)\right] . \tag{2.10}$$

Let us here assume that there is no boundary term in the following integration by parts

$$\int dZ\, d\bar{Z}\, \{e^{tL^T}\mathcal{P}(Z, \bar{Z}; 0)\}\mathcal{O}(Z) = \int dZ\, d\bar{Z}\, \mathcal{P}(Z, \bar{Z}; 0)\{e^{tL}\mathcal{O}(Z)\} , \tag{2.11}$$

4

where the right-hand side is well-defined in the $t \to \infty$ limit. We also assume that the operator $\mathcal{O}(Z)$ is a holomorphic function of Z and that the initial condition is $\mathcal{P}(Z, \bar{Z}; 0) = P(X; 0)\delta(Y)$. Under these assumptions, one can derive (2.7) as

$$
\int dZ \, d\bar{Z} \, \mathcal{P}(Z, \bar{Z}; 0)\{e^{tL}\mathcal{O}(Z)\} = \int dX \, P(X; 0)\{e^{tL_0}\mathcal{O}(X)\}
$$
$$
= \int dX \, \{e^{tL_0^\top} P(X; 0)\}\mathcal{O}(X)
$$
$$
= \int dX \, P(X; t)\mathcal{O}(X) , \tag{2.12}
$$

where we have used $L\mathcal{O}(Z)|_{Y=0} = L_0\mathcal{O}(X)$ for holomorphic $\mathcal{O}(Z)$ and defined

$$
L_0 = \frac{\partial^2}{\partial X^2} + v(X)\frac{\partial}{\partial X} , \qquad L_0^\top = \frac{\partial^2}{\partial X^2} - \frac{\partial}{\partial X}v(X) . \tag{2.13}
$$

Thus the key point in justifying the CLM is the validity of (2.11), which depends on the model as well as its parameter region. There are some criteria [21, 25, 28, 44] for the absence of the boundary term in (2.11). In this paper, we use the one proposed in Ref. [25], which is a practical and convenient criterion based on a sufficient condition for (2.11). This criterion focuses on the probability distribution of the magnitude of the drift term $v(z)$ generated by $\mathcal{P}(Z, \bar{Z}; t)$. If the probability distribution falls off exponentially or faster at large magnitude, the formal expression of the right-hand side in (2.11) is well defined and the boundary term in the integration by parts vanishes.

In practice, we simulate the model with the discretized complex Langevin equation

$$
z(t + \Delta t) = z(t) + v(z(t))\Delta t + \tilde{\eta}(t)\sqrt{\Delta t} , \tag{2.14}
$$

where $\tilde{\eta}(t)$ is generated by the Gaussian distribution $\propto \exp[-\frac{1}{4}\tilde{\eta}(t)^2]$, monitoring the maximum value of the magnitude of the drift term. The expectation value of an observable is obtained by the average of the observable measured at each Langevin time after thermalization. We check the validity criterion by making a histogram for the maximum value of the magnitude of the drift term.

Even when the CLM is supposed to work, it may fail because of some instability in the time-evolution by the discretized complex Langevin equation. This can be controlled by using an adaptive step-size for the discretized time-evolution, which depends on the magnitude of the drift term [19]. In this paper, we choose the step-size Δt such that $\Delta t = \min(\Delta t_0, \Delta t_0 \frac{v_0}{\max(|v(z(t))|)})$, where Δt_0 and v_0 are positive parameters that we set at the beginning of a simulation. Since the model we simulate has more than one dynamical variables, we use $\max(|v(z(t))|)$ for the adaptive step-size, which is the maximum value of the absolute value of the elements of the drift term. Note that one needs to take the adaptive step-size into account when one makes the drift histogram for the criterion.

3 Applying the CLM to the shell model

In this section we apply the CLM reviewed in the previous section to the nuclear shell-model calculations. After defining the shell model, we discuss how it can be investigated by the CLM.

Let us consider a many-body problem of the active particles in the model space, in which the number of the single-particle states and that of the active particles are N_s and N_v, respectively. The many-body shell-model Hamiltonian up to the two-body interaction is written in the density-decomposed form as [8]

$$\hat{H} = \sum_{i,j=1}^{N_s} T_{ij}\, \hat{c}_i^\dagger \hat{c}_j + \frac{1}{2}\sum_\alpha V_\alpha \left(\hat{O}_\alpha\right)^2 \ , \tag{3.1}$$

where $\hat{c}_i^\dagger$ represents the creation operator of a single-particle state and $\hat{O}_\alpha$ represents the density operator of the form $\hat{c}^\dagger \hat{c}$. We have introduced T_{ij}, which denotes the strength of the one-body term, and V_α, which denotes the strength of the two-body interaction.

We simulate this theory at finite temperature by using the standard imaginary-time formalism, where the imaginary time β, which corresponds to the inverse temperature, is sliced up into n_β segments. The partition function for a fixed number N_v of valence nucleons is written as

$$Z = \mathrm{Tr}_{N_v}[(e^{-\Delta\beta\hat{H}})^{n_\beta}] \ , \tag{3.2}$$

where $\Delta\beta = \beta/n_\beta$ and Tr_{N_v} is a trace in the Fock space with N_v particles. Here we use the Hubbard-Stratonovich transformation at each imaginary time to linearize the Hamiltonian with respect to $\hat{O}_\alpha$ by introducing new auxiliary scalar fields $\sigma_{\alpha n}$, where n runs from 1 to n_β. Then the partition function becomes [8]

$$Z = \int [d\sigma]\, (\mathrm{Tr}_{N_v}\hat{U})\, e^{-\frac{1}{2}\Delta\beta \sum_{\alpha n} |V_\alpha|\sigma_{\alpha n}^2} \ , \tag{3.3}$$

$$\hat{U} = e^{-\Delta\beta\hat{h}_{n_\beta}} e^{-\Delta\beta\hat{h}_{n_\beta-1}} \cdots e^{-\Delta\beta\hat{h}_1} \ , \tag{3.4}$$

$$\hat{h}_n = \sum_{i,j} T_{ij}\hat{c}_i^\dagger \hat{c}_j + \sum_\alpha s_\alpha V_\alpha \sigma_{\alpha n}\hat{O}_\alpha \ , \tag{3.5}$$

where $s_\alpha = 1$ for $V_\alpha < 0$ and $s_\alpha = i$ for $V_\alpha > 0$. The integration measure for σ in (3.3) is defined by $[d\sigma] = \prod_{\alpha,n}\left(d\sigma_{\alpha n}\sqrt{\frac{\Delta\beta|V_\alpha|}{2\pi}}\right)$. The expectation value of an observable $\mathcal{O}$ with fixed N_v can be written as

$$\langle \mathcal{O}\rangle_{N_v} = \frac{1}{Z}\int [d\sigma]\frac{\mathrm{Tr}_{N_v}\hat{U}\hat{\mathcal{O}}}{\mathrm{Tr}_{N_v}\hat{U}}(\mathrm{Tr}_{N_v}\hat{U})\, e^{-\frac{1}{2}\Delta\beta\sum_{\alpha n}|V_\alpha|\sigma_{\alpha n}^2} \ . \tag{3.6}$$

Let us call this formalism (3.6) the canonical formalism in this paper.

In fact, the canonical formalism is not very convenient since $\mathrm{Tr}_{N_v} \hat{U}$ takes different forms for different N_v, and it becomes more and more complicated as N_v increases. From this point of view, it is beneficial to rewrite the path integral into the grand canonical ensemble with the number projection [8]. Using the projection onto a fixed N_v given by

$$\delta(\hat{N} - N_v) = \int_0^{2\pi} \frac{d\phi}{2\pi} e^{(\beta\mu + i\phi)(\hat{N} - N_v)} , \qquad (3.7)$$

we rewrite (3.6) as

$$\langle \mathcal{O} \rangle_{N_v} = \frac{1}{Z} \int [d\sigma] \int \frac{d\phi}{2\pi} \mathrm{Tr} \left[e^{(\beta\mu + i\phi)(\hat{N} - N_v)} \hat{U} \hat{\mathcal{O}} \right] e^{-\frac{1}{2} \Delta\beta \sum_{\alpha n} |V_\alpha| \sigma_{\alpha n}^2} ,$$

$$Z = \int [d\sigma] \int \frac{d\phi}{2\pi} \mathrm{Tr} \left[e^{(\beta\mu + i\phi)(\hat{N} - N_v)} \hat{U} \right] e^{-\frac{1}{2} \Delta\beta \sum_{\alpha n} |V_\alpha| \sigma_{\alpha n}^2} , \qquad (3.8)$$

where $\hat{N}$ is the number operator of valence nucleons and μ is the chemical potential. Here Tr is a trace in the entire Fock space of the model space, which sums over all possible N_v. In the CLM, μ is redundant since ϕ is a complex dynamical variable, and therefore we set $\mu = 0$ from now on. It is straightforward to rewrite the weight $\mathrm{Tr}\, e^{i\phi(\hat{N} - N_v)} \hat{U}$ for the grand canonical ensemble by single-particle operators as

$$\mathrm{Tr}\, e^{i\phi(\hat{N} - N_v)} \hat{U} = e^{-i\phi N_v} \det \left(1 + e^{i\phi} U \right) , \qquad (3.9)$$

where U is a one-body matrix defined by $U_{ij} = (\exp[-\beta h^{(\mathrm{tot})}])_{ij}$ with the matrix $h^{(\mathrm{tot})}$ defined by $\hat{U} = \exp[-\beta \sum_{i,j} h_{ij}^{(\mathrm{tot})} \hat{c}_i^\dagger \hat{c}_j]$. Thus, the expectation value in the case of a one-body operator $\hat{\mathcal{O}}$ can be written as

$$\langle \mathcal{O} \rangle_{N_v} = \frac{1}{Z} \int [d\sigma] \int \frac{d\phi}{2\pi} e^{-i\phi N_v} \det \left(1 + e^{i\phi} U \right) e^{-\frac{1}{2} \Delta\beta \sum_{\alpha n} |V_\alpha| \sigma_{\alpha n}^2} \, \mathrm{tr}\, [\mathcal{U}\mathcal{O}] ,$$

$$Z = \int [d\sigma] \int \frac{d\phi}{2\pi} e^{-i\phi N_v} \det \left(1 + e^{i\phi} U \right) e^{-\frac{1}{2} \Delta\beta \sum_{\alpha n} |V_\alpha| \sigma_{\alpha n}^2} , \qquad (3.10)$$

where tr is the matrix trace for $N_s \times N_s$ matrices and we have defined

$$\mathcal{U} = \left(1 + e^{i\phi} U \right)^{-1} e^{i\phi} U . \qquad (3.11)$$

Let us call (3.10) the grand-canonical formalism in this paper.

This formula (3.10) can be generalized to the case in which $\hat{\mathcal{O}}$ is a product of one-body operators $\hat{\mathcal{O}}_1, \cdots, \hat{\mathcal{O}}_n$ using

$$\mathrm{Tr}[e^{i\phi(\hat{N} - N_v)} \hat{U} \hat{\mathcal{O}}_1 \cdots \hat{\mathcal{O}}_n] = e^{-i\phi N_v} \frac{\partial}{\partial \epsilon_1} \cdots \frac{\partial}{\partial \epsilon_n} \det \left(1 + e^{i\phi} U_{\epsilon_1, \cdots, \epsilon_n} \right) \Big|_{\epsilon_1 = \cdots = \epsilon_n = 0} , \qquad (3.12)$$

where $\hat{U}_{\epsilon_1,\cdots,\epsilon_n} = \exp[-\beta \sum_{i,j} h_{ij}^{(\text{tot})} \hat{c}_i^\dagger \hat{c}_j + \sum_{k=1}^n \epsilon_k \hat{\mathcal{O}}_k]$ corresponding to a one-body matrix $(U_{\epsilon_1,\cdots,\epsilon_n})_{ij} = (\exp[-\beta h^{(\text{tot})} + \sum_k \epsilon_k \mathcal{O}_k])_{ij}$. For instance, the energy (3.1), which involves two-body operators, can be written as

$$\langle H \rangle_{N_v} = \frac{1}{Z} \int [d\sigma] \int d\phi \, e^{-i\phi N_v} \det\left(1 + e^{i\phi} U\right) e^{-\frac{1}{2}\Delta\beta \sum_{\alpha n} |V_\alpha| \sigma_{\alpha n}^2}$$

$$\times \left(\text{tr}\,[\mathcal{U}T] + \frac{1}{2} \sum_\alpha V_\alpha \left\{ (\text{tr}\,[\mathcal{U}O_\alpha])^2 + \text{tr}\,[\mathcal{U}O_\alpha^2] - \text{tr}\,[\mathcal{U}O_\alpha \mathcal{U}O_\alpha] \right\} \right) . \quad (3.13)$$

The standard procedure in the literature is to reduce the integration over ϕ to a summation over N_s integers [8]. In the CLM, however, we leave the integration over ϕ as it is and treat ϕ as another integration variable.

In our simulations, we change the normalization of the variables as $\sigma_{\alpha n} = \frac{\tilde{\sigma}_{\alpha n}}{\sqrt{\Delta\beta |V_\alpha|}}$. The effective action then becomes

$$S = \sum_{\alpha,n} \frac{\tilde{\sigma}_{\alpha n}^2}{2} - \ln \det\left[1 + e^{i\phi} U\right] + i N_v \phi . \quad (3.14)$$

Using this effective action, the Langevin equations are obtained as

$$\frac{d\tilde{\sigma}_{\alpha n}}{dt} = -\frac{\partial S}{\partial \tilde{\sigma}_{\alpha n}} + \eta_{\alpha n}(t), \qquad \frac{d\phi}{dt} = -\frac{\partial S}{\partial \phi} + \eta_\phi(t) , \quad (3.15)$$

where $\eta_{\alpha n}$ and η_ϕ represent the Gaussian noise, which satisfies $\langle \eta_{\alpha n}(t) \eta_{\beta m}(0) \rangle = 2\delta_{\alpha\beta}\delta_{nm}\delta(t)$ and $\langle \eta_\phi(t) \eta_\phi(0) \rangle = 2\delta(t)$. The drift terms are calculated as

$$\frac{\partial S}{\partial \tilde{\sigma}_{\alpha n}} = \tilde{\sigma}_{\alpha n} - \text{tr}\left[\left(1 + e^{i\phi}U\right)^{-1} e^{i\phi} \frac{\partial U}{\partial \tilde{\sigma}_{\alpha n}}\right] = \tilde{\sigma}_{\alpha n} - \text{tr}\left[\mathcal{U}U^{-1} \frac{\partial U}{\partial \tilde{\sigma}_{\alpha n}}\right] ,$$

$$\frac{\partial S}{\partial \phi} = -i\,\text{tr}\left[\left(1 + e^{i\phi}U\right)^{-1} e^{i\phi}U\right] + i N_v = -i\left(\text{tr}\,[\mathcal{U}] - N_v\right) . \quad (3.16)$$

See Appendix A for the implementation of the canonical formalism in the CLM.

The computational cost for the grand-canonical formalism[1] grows as $O((N_s)^5 n_\beta)$. The dominant part comes from the calculation of the drift terms (3.16) in the complex Langevin equation, which contains the calculations of U, $\mathcal{U}$ and $\frac{\partial U}{\partial \tilde{\sigma}_{\alpha n}}$. The calculation of U involves matrix multiplications in the imaginary-time direction, which cost $O((N_s)^3 n_\beta)$. The calculation of $\mathcal{U}$ involves taking the inverse of $N_s \times N_s$ matrices, which costs $O((N_s)^3)$. The most dominant part comes from the calculation of $\frac{\partial U}{\partial \tilde{\sigma}_{\alpha n}}$ since it involves matrix multiplications at each $\alpha = 1, \cdots, N_\alpha$, which costs $O(N_\alpha (N_s)^3 n_\beta)$. Using $N_\alpha = (N_s)^2$, which is the case in our implementation, the computational cost becomes $O((N_s)^5 n_\beta)$.

---

[1]The computational cost for the canonical formalism is $O((N_s)^5 n_\beta)$ as well since the calculation of $\frac{\partial U}{\partial \tilde{\sigma}_{\alpha n}}$ appears in the drift term (A.4).
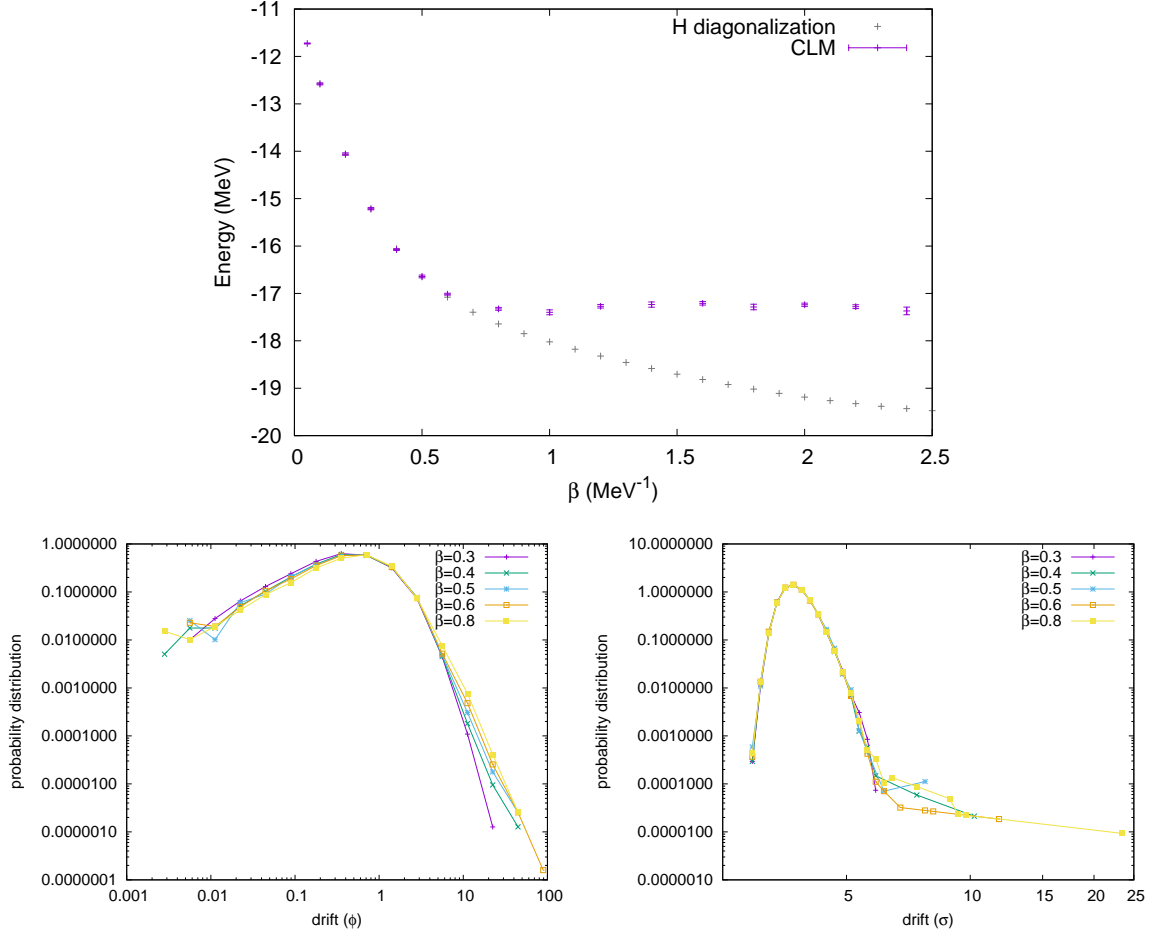
8

Figure 1: (Top) The expectation value of the energy is plotted against the inverse temperature β in the grand-canonical formalism with $N_s = 20$, $N_v = 2$, $n_\beta = 10$. The purple points with error bars represent the CLM results, whereas the gray points represent the data obtained by the Hamiltonian diagonalization. (Bottom) The drift histogram for the ϕ field (Left) and the σ field (Right).

4   The results of the CLM

In this section, we present our numerical results for the shell model obtained by the CLM. We focus on the case with $N_s = 20$ in the pf shell, considering only valence neutrons for simplicity. The interaction we use in the Hamiltonian (3.1) is taken from GXPF1A in Ref. [45]. Throughout this paper, we set the Langevin step-size to $\Delta t = 5 \times 10^{-3}$, which is found to be small enough for the accuracy required in this paper.
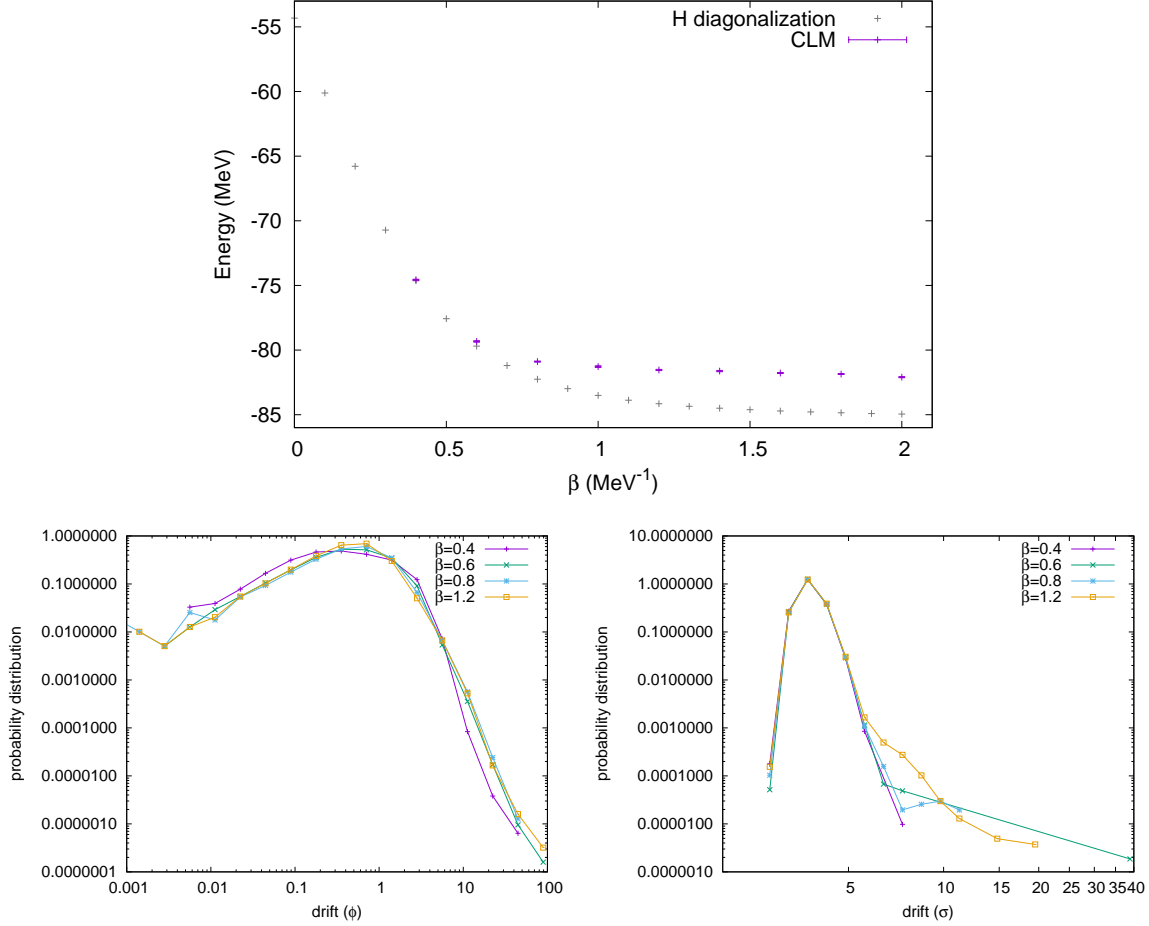
Figure 2: Similarly to Fig. 1, we present the results for the grand-canonical formalism with $N_s = 20$, $N_v = 10$, $n_\beta = 10$.

4.1   Dependence on the temperature

Let us discuss how our results depend on the temperature. In Fig. 1, we show our results for $N_v = 2$ in the grand-canonical formalism with various inverse temperature β. The number of steps in the imaginary time direction is set to $n_\beta = 10$. In the Top panel, we plot the expectation value of the energy in units of MeV against β in units of MeV^{-1}. We observe good agreement with the results obtained by the Hamiltonian diagonalization for $\beta \lesssim 0.6$. On the other hand, the energy ceases to decrease monotonically for $\beta \gtrsim 0.6$, which represents an unphysical behavior.

In the Bottom panel, we show the histogram of the drift terms. Since the histogram for $\beta = 0.3$ seems to fall off exponentially for both ϕ and σ fields, we can safely say that the CLM for $\beta \lesssim 0.3$ is justified, which is consistent with the agreement with the

10

results of the Hamiltonian diagonalization in that region. On the other hand, the drift histogram for the σ field does not show a fast fall-off for $\beta \gtrsim 0.4$, which suggests that the agreement with the results of the Hamiltonian diagonalization in the $0.4 \lesssim \beta \lesssim 0.6$ is rather accidental.

Let us recall that the grand-canonical formalism allows us to obtain results for different N_v in a straightforward manner unlike the canonical formalism. In Fig. 2 we show our results for $N_v = 10$ with $n_\beta = 10$. We observe good agreement with the result of the Hamiltonian diagonalization for $\beta \lesssim 0.4$, which is consistent with the result of the drift histogram.

As we have seen above, the CLM works only at sufficiently small β (high temperature), at least for the $N_s = 20$ case with valence neutrons. However, if we are interested in the ground state energy, we have to take the $\beta \to \infty$ limit. Since the result for finite β is a weighted sum over the low-lying energy levels E_n with the Boltzmann weight $e^{-\beta E_n}$, it is not straightforward to extract the energy levels E_n from the observed β dependence of the energy expectation values.

4.2   Extrapolation with respect to the interaction term

In this section, we attempt to extract the results for larger β (lower temperature) by introducing an additional parameter and making an extrapolation.[2]

Here we introduce a tunable parameter t in the Hamiltonian (3.1) as

$$\hat{H}_t = \sum_{i,j} T_{ij} \hat{c}_i^\dagger \hat{c}_j + \frac{t}{2} \sum_\alpha V_\alpha \left(\hat{O}_\alpha \right)^2 . \tag{4.1}$$

Since the observables at small t is described by perturbation theory around $t = 0$, it is given by a polynomial in t in that region. Hence we can make an extrapolation to $t = 1$ using a polynomial as a natural fitting ansatz.

In Fig. 3 (Top-Left), we plot the expectation value of the energy against the tunable parameter t for $N_v = 2$ and $\beta = 1$ in the canonical and grand-canonical formalisms with $n_\beta = 10$. We find good agreement with the result of the Hamiltonian diagonalization for $t \lesssim 0.6$. The drift histogram indicates that the region of validity is $t \lesssim 0.4$ for the grand-canonical formalism and $t \lesssim 0.5$ for the canonical formalism.

---

[2]This is analogous to the g-extrapolation [10], where one deforms the system by multiplying a real parameter g to all the interaction terms in the Hamiltonian (3.1) with $V_\alpha > 0$ so that the sign problem disappears for $g < 0$. Then the desired expectation value is obtained by extrapolating the data for $g < 0$ to $g = 1$.
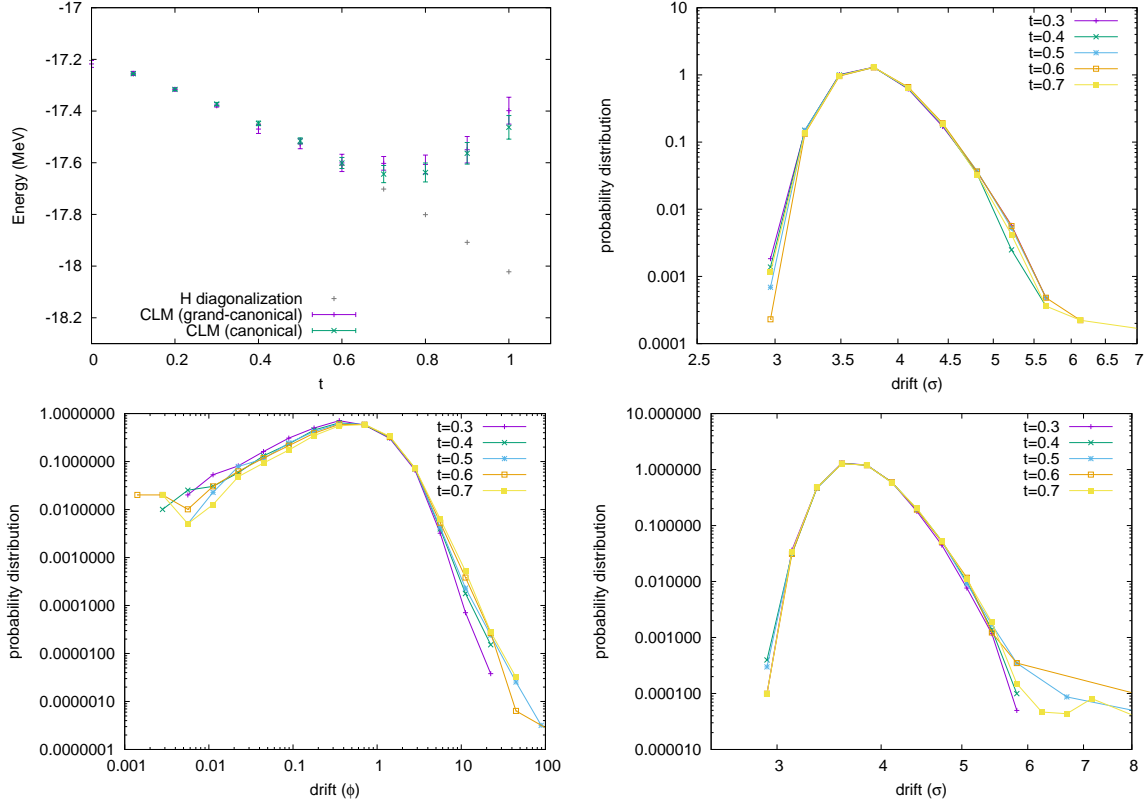
Figure 3: (Top-Left) The expectation value of the energy is plotted against the tunable parameter t in the canonical and grand-canonical formalisms with $N_s = 20$, $N_v = 2$, $\beta = 1$, $n_\beta = 10$. (Top-Right) The drift histogram for the σ field in the canonical formalism. (Bottom) The drift histogram for the ϕ field (Left) and the σ field (Right) in the grand-canonical formalism.

We fit these data in these regions to a quadratic function in Fig. 4. The fitting curve obtained in this way is consistent with the result obtained by the Hamiltonian diagonalization within the fitting errors up to the target value $t = 1$. Thus we can obtain the expectation value of the energy at $\beta = 1$. Let us note that the difference of the energy of the ground state and the first excited state is $\delta E \sim 1.438(\text{MeV})$ in the present case, which means that $e^{-\beta \delta E} \sim 0.237 \cdots$. In order to extract the ground state energy, it would be desirable to obtain results up to $\beta \sim 3$. The fitting ansatz in such cases would need high orders in t, which makes the extrapolation less reliable.
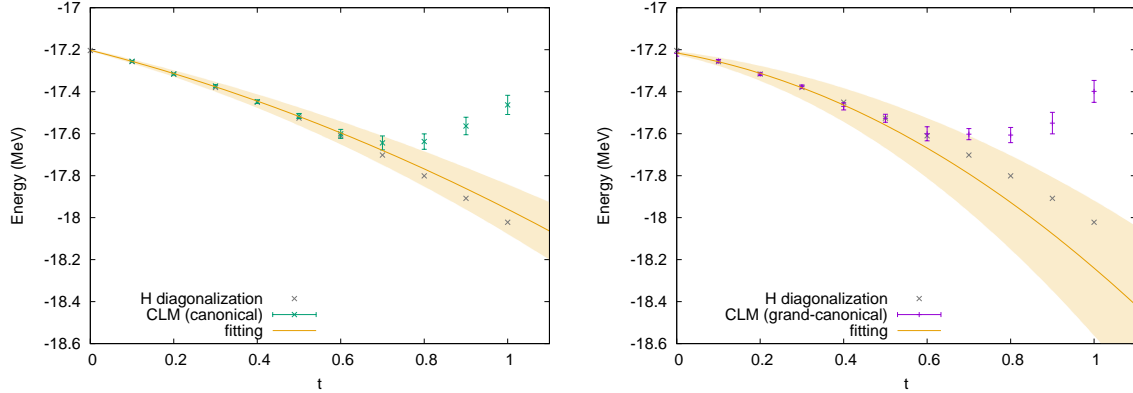
Figure 4: The expectation value of the energy is plotted against the tunable parameter t for the canonical (Left) and grand-canonical (Right) formalisms, with $N_s = 20$, $N_v = 2$, $\beta = 1$ and $n_\beta = 10$. The solid orange line represents a fit to a quadratic function, using the data within $0 \leq t \leq 0.5$ for the canonical formalism and the data within $0 \leq t \leq 0.4$ for the grand-canonical formalism. The shaded region represents the fitting errors. The crosses represent the results obtained by the Hamiltonian diagonalization, which are consistent with the fitting curves within the fitting errors.

5   Summary

We have discussed how the nuclear shell model can be investigated without the variational ansatz by applying the CLM, which overcomes the sign problem in quantum Monte Carlo methods. In particular, we find that the grand-canonical formalism (3.10) is convenient to simulate the case with various N_v including the region $N_v \sim N_s/2$, where the canonical formalism (3.6) becomes too complicated to implement.

As a first step, we have performed explicit calculations for $^{40+N_v}$Ca systems ($N_s = 20$), with a realistic potential at finite temperature. Our results agree with the results of the Hamiltonian diagonalization at high temperature but not at low temperature. This has been understood from the viewpoint of the validity criterion [25], which is a sufficient condition for the correct convergence of the CLM. The temperature at which the agreement ceases to hold is slightly lower than the temperature at which the drift histogram starts to have a slow fall-off. Thus by probing the drift histogram, we can safely estimate the validity region of the CLM calculations.

In order to obtain results at lower temperature, which is not directly accessible by the CLM, we have proposed to introduce a tunable parameter t in the interaction terms so that the original Hamiltonian is obtained at $t = 1$. In the case we studied, the region of t

in which the CLM works is large enough to make an extrapolation to $t = 1$ by a quadratic fit. The result obtained by this extrapolation is consistent with the result obtained by the Hamiltonian diagonalization within the fitting errors. The extrapolation turns out to be easier for the canonical formalism (3.6) than the grand-canonical formalism (3.10) due to a slightly larger validity region of the CLM.

For heavier nuclei, the computational cost increases as $\sim (N_s)^5 (N_v)^0 n_\beta$ as we discussed at the end of section 3. While the sign problem becomes severer, it is possible that the validity region of the CLM is not significantly affected by the system size. We therefore expect that the CLM can be a useful approach to heavy nuclei, which is complementary to the variational method.

Acknowledgment

A   Canonical formalism

In this appendix, we discuss how to implement the canonical formalism in the CLM. As we did for the grand-canonical formalism, we change variables as $\sigma_{\alpha n} = \frac{\tilde{\sigma}_{\alpha n}}{\sqrt{\Delta \beta |V_\alpha|}}$ for simplicity.

We can write the effective action of the path integral (3.3) as

$$S = \sum_{\alpha,n} \frac{\tilde{\sigma}_{\alpha n}^2}{2} - \ln \mathrm{Tr}_{N_v} \hat{U} \ . \tag{A.1}$$

The complex Langevin equation is then written as

$$\frac{d\tilde{\sigma}_{\alpha n}}{dt} = -\frac{\partial S}{\partial \tilde{\sigma}_{\alpha n}} + \eta_{\alpha n}(t) \ , \tag{A.2}$$

where $\eta_{\alpha n}$ is a Gaussian noise term that satisfies $\langle \eta_{\alpha n}(t) \eta_{\beta m}(0) \rangle = 2\delta_{\alpha\beta}\delta_{nm}\delta(t)$.

Unlike the grand-canonical formalism, the effective action (A.1) involves a trace in the subspace of the Fock space with N_v particles. Therefore, in order to derive a more explicit

14

form of the drift term, we need to specify the value of N_v and to transform Tr_{N_v} into an expression written in terms of matrix traces. For instance, in the case of $N_v = 2$, $\text{Tr}_2 \hat{U}$ can be rewritten as

$$\text{Tr}_2 \hat{U} = \frac{1}{2} \left[(\text{tr}\, U)^2 - \text{tr}\, U^2 \right] \, , \tag{A.3}$$

where U is the one-body matrix defined by $U_{ij} = (\exp[-\beta h^{(\text{tot})}])_{ij}$, and the drift term becomes

$$\frac{\partial S}{\partial \tilde{\sigma}_{\alpha n}} = \tilde{\sigma}_{\alpha n} - \frac{2}{(\text{tr}\, U)^2 - \text{tr}\, U^2} \, \text{tr} \left[(\text{tr}\, U) \frac{\partial U}{\partial \tilde{\sigma}_{\alpha n}} - \left(U \frac{\partial U}{\partial \tilde{\sigma}_{\alpha n}} \right) \right] \, . \tag{A.4}$$

The derivative of U with respect to $\tilde{\sigma}_{\alpha n}$ is written explicitly as

$$\frac{\partial U}{\partial \tilde{\sigma}_{\alpha n}} = s_\alpha^* \sqrt{\Delta\beta |V_\alpha|} e^{-\Delta\beta h_{n_\beta}} \cdots e^{-\Delta\beta h_{n+1}} \left(\frac{e^{-\Delta\beta\, \text{adj}\, h_n} - 1}{-\Delta\beta\, \text{adj}\, h_n} O_\alpha \right) e^{-\Delta\beta h_n} \cdots e^{-\Delta\beta h_1} \, , \tag{A.5}$$

where $\hat{h}_n = \sum_{i,j} (h_n)_{ij} \hat{c}_i^\dagger \hat{c}_j$ and $\hat{O}_\alpha = \sum_{i,j} (O_\alpha)_{ij} \hat{c}_i^\dagger \hat{c}_j$. We have defined an operation $(\text{adj}\, A)\, B \equiv [A, B]$. The appearance of s_α^* is due to the use of the relation $s_\alpha V_\alpha = -s_\alpha^* |V_\alpha|$. By diagonalizing h_n as $(P_n^{-1} h_n P_n)_{ij} = \lambda_{n,i} \delta_{ij}$, we can rewrite the factor with O_α into an explicit form

$$\left(\frac{e^{-\Delta\beta\, \text{adj}\, h_n} - 1}{-\Delta\beta\, \text{adj}\, h_n} O_\alpha \right)_{ij} = \sum_{i',j'} (P_n)_{ii'} \frac{e^{-\Delta\beta(\lambda_{n,i'} - \lambda_{n,j'})} - 1}{-\Delta\beta(\lambda_{n,i'} - \lambda_{n,j'})} (P_n^{-1} O_\alpha P_n)_{i'j'} (P_n^{-1})_{j'j} \, . \tag{A.6}$$

References

[1] T. Otsuka, A. Gade, O. Sorlin, T. Suzuki and Y. Utsuno, *Evolution of shell structure in exotic nuclei*, Rev. Mod. Phys. **92** (2020) 015002.

[2] E. Caurier, G. Martinez-Pinedo, F. Nowacki, A. Poves and A.P. Zuker, *The shell model as a unified view of nuclear structure*, Rev. Mod. Phys. **77** (2005) 427.

[3] N. Tsunoda, T. Otsuka, K. Takayanagi, N. Shimizu, T. Suzuki, Y. Utsuno et al., *The impact of nuclear shape on the emergence of the neutron dripline*, Nature **587** (2020) 66.

[4] Y. Alhassid, G.F. Bertsch and L. Fang, *Nuclear level statistics: Extending shell model theory to higher temperatures*, Phys. Rev. C **68** (2003) 044322.

[5] N. Shimizu, T. Mizusaki, Y. Utsuno and Y. Tsunoda, *Thick-restart block Lanczos method for large-scale shell-model calculations*, Computer Physics Communications **244** (2019) 372.

[6] T. Otsuka, M. Honma, T. Mizusaki, N. Shimizu and Y. Utsuno, *Monte Carlo shell model for atomic nuclei*, *Prog. Part. Nucl. Phys.* **47** (2001) 319 .

[7] K.W. Schmid, Z. R.-Rong, F. Grummer and A. Faessler, *Beyond symmetry-projected quasi-particle mean fields: A new variational procedure for nuclear structure calculations*, *Nucl. Phys. A* **499** (1989) 63.

[8] S. Koonin, D. Dean and K. Langanke, *Shell model Monte Carlo methods*, *Phys. Rept.* **278** (1997) 1 .

[9] H. Hergert, S. Bogner, T. Morris, A. Schwenk and K. Tsukiyama, *The in-medium similarity renormalization group: A novel ab initio method for nuclei*, *Phys. Rept.* **621** (2016) 165.

[10] Y. Alhassid, D.J. Dean, S.E. Koonin, G. Lang and W.E. Ormand, *Practical solution to the Monte Carlo sign problem: Realistic calculations of ^{54}Fe*, *Phys. Rev. Lett.* **72** (1994) 613.

[11] K. Langanke, J. Terasaki, F. Nowacki, D.J. Dean and W. Nazarewicz, *How magic is the magic ^{68}Ni nucleus?*, *Phys. Rev. C* **67** (2003) 044314.

[12] C. Özen, Y. Alhassid and H. Nakada, *Nuclear state densities of odd-mass heavy nuclei in the shell model Monte Carlo approach*, `1304.7405`.

[13] J. Bonnard and O. Julilet, *Constrained-Path Quantum Monte Carlo Approach for the Nuclear Shell Model*, *Phys. Rev. Lett.* **111** (2013) 012502.

[14] K.W. Schmid, *Large scale nuclear structure calculations with VAMPIR*, *Prog. Part. Nucl. Phys.* **46** (2001) 145.

[15] N. Shimizu, T. Abe, M. Honma, T. Otsuka, T. Togashi, Y. Tsunoda et al., *Monte Carlo shell model studies with massively parallel supercomputers*, *Physica Scripta* **92** (2017) 063001.

[16] G. Parisi, *On Complex Probabilities*, *Phys. Lett. B* **131** (1983) 393.

[17] J.R. Klauder, *Coherent State Langevin Equations for Canonical Quantum Systems With Applications to the Quantized Hall Effect*, *Phys. Rev. A* **29** (1984) 2036.

[18] C. Adami and S.E. Koonin, *Complex langevin equation and the many-fermion problem*, *Phys. Rev. C* **63** (2001) [`nucl-th/0009021`].

[19] G. Aarts, F.A. James, E. Seiler and I.-O. Stamatescu, *Adaptive stepsize and instabilities in complex Langevin dynamics*, *Phys. Lett. B* **687** (2010) 154 [0912.0617].

[20] G. Aarts, E. Seiler and I.-O. Stamatescu, *The Complex Langevin method: When can it be trusted?*, *Phys. Rev. D* **81** (2010) 054508 [0912.3360].

[21] G. Aarts, F.A. James, E. Seiler and I.-O. Stamatescu, *Complex Langevin: Etiology and Diagnostics of its Main Problem*, *Eur. Phys. J. C* **71** (2011) 1756 [1101.3270].

[22] E. Seiler, D. Sexty and I.-O. Stamatescu, *Gauge cooling in complex Langevin for QCD with heavy quarks*, *Phys. Lett. B* **723** (2013) 213 [1211.3709].

[23] J. Nishimura and S. Shimasaki, *New Insights into the Problem with a Singular Drift Term in the Complex Langevin Method*, *Phys. Rev. D* **92** (2015) 011501 [1504.08359].

[24] K. Nagata, J. Nishimura and S. Shimasaki, *Justification of the complex Langevin method with the gauge cooling procedure*, *Prog. Theor. Exp. Phys.* **2016** (2016) 013B01 [1508.02377].

[25] K. Nagata, J. Nishimura and S. Shimasaki, *Argument for justification of the complex Langevin method and the condition for correct convergence*, *Phys. Rev. D* **94** (2016) 114515 [1606.07627].

[26] Y. Ito and J. Nishimura, *The complex Langevin analysis of spontaneous symmetry breaking induced by complex fermion determinant*, *JHEP* **12** (2016) 009 [1609.04501].

[27] G. Aarts, E. Seiler, D. Sexty and I.-O. Stamatescu, *Complex Langevin dynamics and zeroes of the fermion determinant*, *JHEP* **05** (2017) 044 [1701.02322].

[28] M. Scherzer, E. Seiler, D. Sexty and I.-O. Stamatescu, *Complex Langevin and boundary terms*, *Phys. Rev. D* **99** (2019) 014512 [1808.05187].

[29] D. Sexty, *Simulating full QCD at nonzero density using the complex Langevin equation*, *Phys. Lett.* **B729** (2014) 108 [1307.7748].

[30] G. Aarts, E. Seiler, D. Sexty and I.-O. Stamatescu, *Simulating QCD at nonzero baryon density to all orders in the hopping parameter expansion*, *Phys. Rev.* **D90** (2014) 114505 [1408.3770].

[31] Z. Fodor, S. Katz, D. Sexty and C. Torok, *Complex Langevin dynamics for dynamical QCD at nonzero chemical potential: A comparison with multiparameter reweighting*, Phys. Rev. D **92** (2015) 094516 [1508.05260].

[32] K. Nagata, J. Nishimura and S. Shimasaki, *Complex Langevin calculations in finite density QCD at large μ/T with the deformation technique*, Phys. Rev. **D98** (2018) 114513 [1805.03964].

[33] J.B. Kogut and D.K. Sinclair, *Applying complex Langevin simulations to lattice QCD at finite density*, Phys. Rev. **D100** (2019) 054512 [1903.02622].

[34] D. Sexty, *Calculating the equation of state of dense quark-gluon plasma using the complex Langevin equation*, Phys. Rev. D **100** (2019) 074503 [1907.08712].

[35] S. Tsutsui, Y. Ito, H. Matsufuru, J. Nishimura, S. Shimasaki and A. Tsuchiya, *Exploring the QCD phase diagram at finite density by the complex Langevin method on a $16^3 \times 32$ lattice*, in *37th International Symposium on Lattice Field Theory (Lattice 2019) Wuhan, Hubei, China, June 16-22, 2019*, 2019 [1912.00361].

[36] M. Scherzer, D. Sexty and I.O. Stamatescu, *Deconfinement transition line with the complex Langevin equation up to $\mu/T \sim 5$*, Phys. Rev. D **102** (2020) 014515 [2004.05372].

[37] Y. Ito, H. Matsufuru, Y. Namekawa, J. Nishimura, S. Shimasaki, A. Tsuchiya et al., *Complex Langevin calculations in QCD at finite density*, JHEP **10** (2020) 144 [2007.08778].

[38] S. Tsutsui, Y. Asano, Y. Ito, H. Matsufuru, Y. Namekawa, J. Nishimura et al., *On the validity of the complex Langevin method near the deconfining phase transition in QCD at finite density*, 2505.06551.

[39] C.E. Berger, L. Rammelmüller, A.C. Loheac, F. Ehmann, J. Braun and J.E. Drut, *Complex Langevin and other approaches to the sign problem in quantum many-body physics*, Phys. Rept. **892** (2021) 1 [1907.10183].

[40] F. Attanasio, B. Jäger and F.P.G. Ziegler, *Complex Langevin simulations and the QCD phase diagram: Recent developments*, Eur. Phys. J. A **56** (2020) 251 [2006.00476].

[41] K. Nagata, *Finite-density lattice QCD and sign problem: Current status and open problems*, Prog. Part. Nucl. Phys. **127** (2022) 103991 [2108.12423].

[42] A. Yamamoto and T. Hayata, *Complex langevin simulation in condensed matter physics*, *PoS (LATTICE 2015) 041* (2015) [1508.00415].

[43] P. Navratil, S. Quaglioni, I. Stetcu and B.R. Barrett, *Recent developments in no-core shell-model calculations*, *Journal of Physics G: Nuclear and Particle Physics* **36** (2009) 083101.

[44] L.L. Salcedo, *Does the complex Langevin method give unbiased results?*, *Phys. Rev. D* **94** (2016) 114505 [1611.06390].

[45] M. Honma, T. Otsuka, B.A. Brown and T. Mizusaki, *Shell-model description of neutron-rich pf-shell nuclei with a new effective interaction GXPF 1*, *Eur. Phys. J. A* **25** (2005) 499.